

S.M. HUANG<sup>✉</sup>  
M.H. HONG  
B. LUKIYANCHUK  
T.C. CHONG

# Nanostructures fabricated on metal surfaces assisted by laser with optical near-field effects

Laser Microprocessing Laboratory, Data Storage Institute and Department of Electrical and Computer Engineering, National University of Singapore, Singapore 117608

Received: 10 December 2002/Accepted: 20 January 2003  
Published online: 28 May 2003 • © Springer-Verlag 2003

**ABSTRACT** Nanostructures on metal film surfaces have been written directly using a pulsed ultraviolet laser. The optical near-field effects of the laser were investigated. Spherical silica particles (500–1000 nm in diameter) were placed on metal films. After laser illumination with a single laser shot, nanoholes were obtained at the original position of the particles. The mechanism for the formation of the nanostructure patterns was investigated and found to be the near-field optical resonance effect induced by the particles on the surface. The size of the nanohole was studied as a function of laser fluence and silica particle size. The experimental results show a good agreement with those of the relevant theoretical calculations of the near-field light intensity distribution. The method of particle-enhanced laser irradiation allows the study of field enhancement effects as well as its potential applications for nanolithography.

PACS 81.16.Mk; 61.80.Ba; 81.16.Rf; 81.65.Cf

## 1 Introduction

The current trend towards sub-micrometer structures creates a need for new methods and technologies of surface structuring. Intense research has been attracted to this trend. As optical lithography using the traditional masking approach is limited by diffraction effects and is characterized by complex systems and high costs, a lot of alternative techniques have been developed. One approach in this respect consists of the illumination of the tip of a scanning tunneling microscope (STM) or the tip of an atomic force microscope (AFM) with a pulsed laser. Structures with lateral dimensions below 10 nm, and therefore well below a half-wavelength of the laser ( $\alpha/2$ ), could be produced underneath the tip [1–5]. It was proposed that the enhancement of the electromagnetic field in the vicinity of the tip and the thermal expansion of the tip were responsible for this effect [4–9]. Thus, both setups seemed to be promising for the study of field enhancement effects at sharp tips, a question of great interest in optics and surface structuring applications.

Another approach involves the illumination of micrometer- and sub-micrometer-sized spheres, which will likely

allow the study of field enhancement effects, as well as its application to nanolithography processes. Some authors have reported the appearance of particle-induced damage on the irradiated surface area during dry laser cleaning of irregularly shaped  $\text{Al}_2\text{O}_3$  particles from glass [10, 11]. Recent experiments have shown that, using a femtosecond or nanosecond pulsed laser, the great light enhancement on the hot spot can produce a small pit on a silicon substrate [12, 13]. It is known [14] that spherical particles may act as spherical lenses, and therefore increase the laser intensity, if their diameters are bigger than the laser wavelength. If their diameters are smaller than the wavelength, field enhancement at the particles may happen according to Mie theory. In this study, nanostructure fabrication on nickel surfaces was investigated using particle-enhanced laser irradiation. Pit arrays were created. The dependence of the apparent diameters and depths of the pits on particle size parameter or laser intensity was investigated. The morphologies of the created features were characterized by AFM and scanning electron microscopy (SEM). Theoretical calculations and an accurate solution of the boundary-value problem indicate that the incident light could excite some resonance modes inside the particles and produce enhanced light intensities near the contact area. These calculation results give a good explanation of the experimental phenomena in laser-assisted structuring of the surface as presented in the following sections.

## 2 Experimental details

Monodisperse silica ( $\text{SiO}_2$ ) (Duke Scientific Corp.) with diameters in the range of 500 nm to 1000 nm were used. These particles are transparent to ultraviolet (UV) light. Colloidal particles can be deposited onto various materials, including polymeric, biological, and semiconducting ones. Hexagonally closed-packed colloidal monolayers can be directly prepared on the surface by a spin-coating process or in a self-organizing process. The relevant techniques have been described in detail in [15, 16]. In this work, we wanted to concentrate on studying the mechanism for the formation of nanostructures on a surface and on investigating optical resonance and near-field effects in the interaction of transparent particle on a substrate with laser light. In the preparation of our samples, monodisperse  $\text{SiO}_2$  spheres with different sizes were applied to the sample after the particle suspension

✉ Fax: +65-777/1349, E-mail: HUANG\_Sumei@dsi.a-star.edu.sg

had been rarefied with deionized (DI) water. Isolated spheres at any desired concentration on the sample were deposited on the sample by controlling the application of a colloidal suspension. Nickel films on silicon substrates were used as samples. The films were deposited by a hot evaporator on the Si substrates. The light source was a KrF excimer laser with a wavelength of 248 nm and a pulse width of 23 ns. The laser fluence was in the range of 100 to 500 mJ/cm<sup>2</sup>. The 25 mm × 5 mm rectangular laser spot had a uniform light intensity. Compared with other lasers such as femtosecond lasers, excimer lasers have larger beam sizes. The laser beam was incident normally on the sample with particles on the surface. Each sample was treated using a single laser pulse. The surfaces before and after laser treatment were observed with a high-resolution optical microscope. During the laser irradiation, we found that most of particles could be removed from the sample surface. The sample was ultrasonically cleaned before AFM and SEM measurements were done.

### 3 Results and discussion

Two kinds of SiO<sub>2</sub> colloids were mixed and applied to the sample. The diameters of the SiO<sub>2</sub> particles of one colloid were 0.95 μm, with a standard deviation of less than ±10%. The diameters of the SiO<sub>2</sub> particles of the other colloid were 0.47 μm, with a standard deviation of less than ±10%. Figure 1 shows an AFM image of the particle distribution on a Ni film after water was evaporated in air. From Fig. 1, particles with sizes of about 0.5 and 1.0 μm in diameter were monodispersely distributed on the sample surface, and SiO<sub>2</sub> particles with the same size tended to be arrayed in lines. Figure 2a displays a typical SEM morphology of pits formed after laser irradiation of the colloidal monodisperse layer on the Ni surface with a single pulse. The laser fluence was 400 mJ/cm<sup>2</sup>. With higher magnifications, the pits formed are more clearly shown in Figs. 2b and c. From Figs. 2a–c, the positions of the pits reflect the previous positions of the

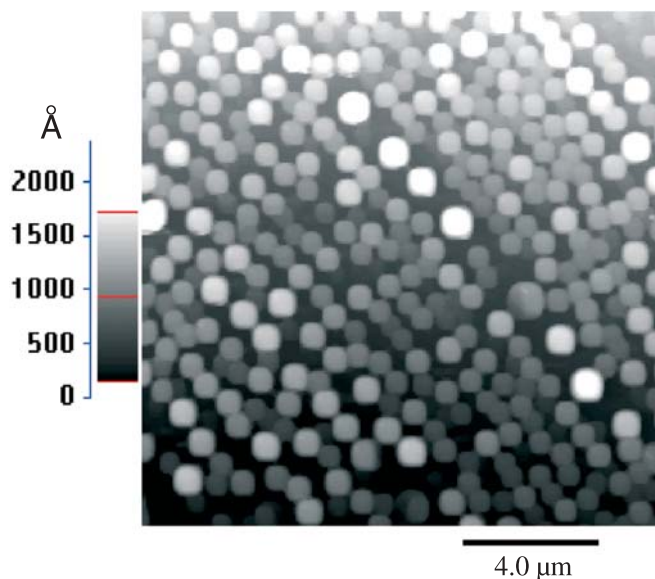


**FIGURE 1** AFM image of isolated particles on a Ni surface before laser irradiation

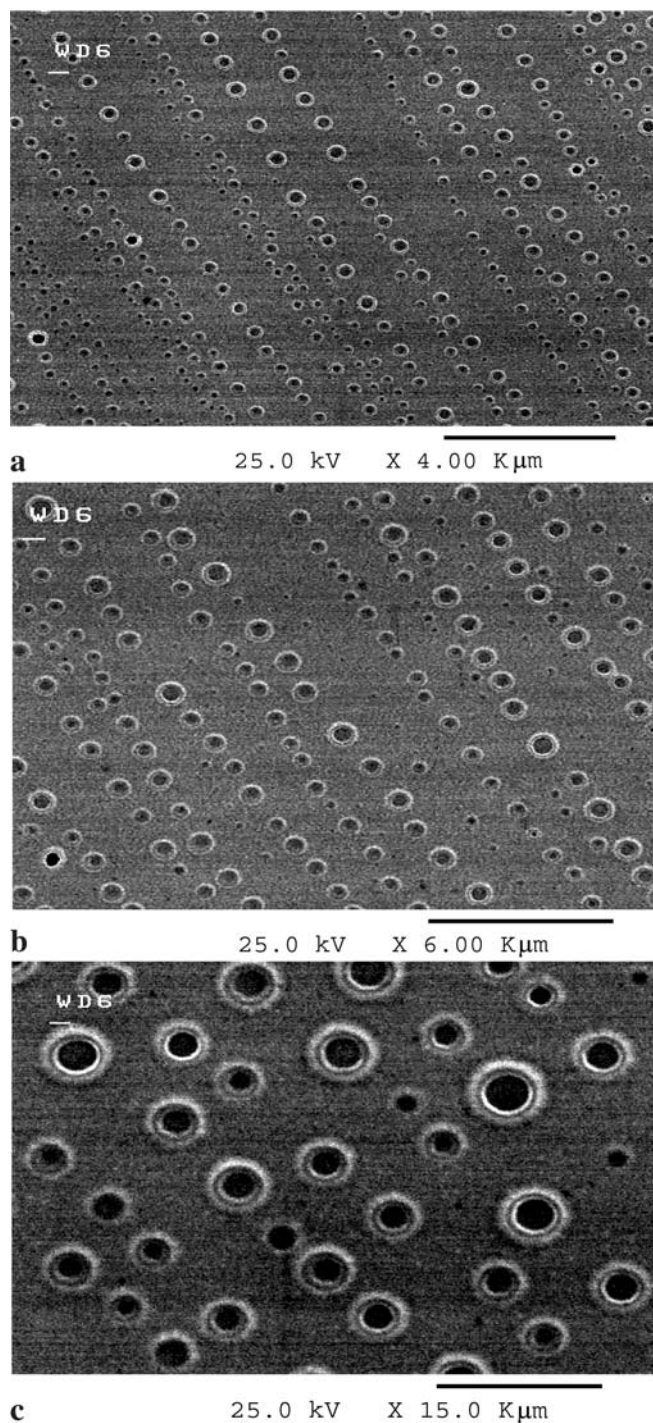


**FIGURE 2** SEM images of pits formed after illumination of isolated particles on a Ni surface by a single pulse with a laser fluence of 400 mJ/cm<sup>2</sup>

colloid spheres and also show linear arrays similar to those shown in Fig. 1. The pits show halo profiles. As we can see in Fig. 2, the diameter of the small hole created by an approximately 0.5-μm particle was about 250 nm, and its depth was about 20 nm, according to AFM analysis. The size distribution of the resultant holes appears to be rather broad. This can be attributed to the large variations and deviations in particle size shown in Fig. 1. The diameter of the large hole created by an approximately 1.0-μm particle was about 470 nm, and its depth was about 34 nm, according to AFM analysis. With

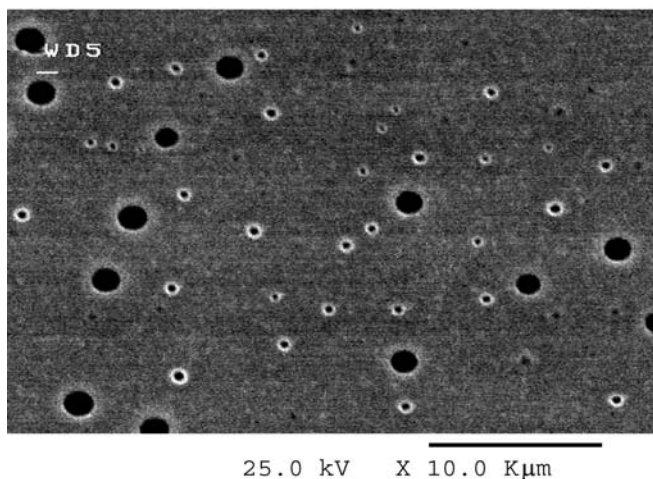


**FIGURE 3** SEM images of pits formed after irradiation of isolated particles on a Ni surface by a single pulse with a laser fluence of  $150 \text{ mJ/cm}^2$

a lower laser fluence of  $150 \text{ mJ/cm}^2$ , shallower and smaller holes could also be created for each particle size. Figure 3 shows a typical SEM morphology of pit arrays with this laser fluence. The diameter of the small hole created by an approximately  $0.5\text{-}\mu\text{m}$  particle was about  $150 \text{ nm}$ , and its depth was about  $3.0 \text{ nm}$ . The diameter of the large hole created by an approximately  $1.0\text{-}\mu\text{m}$  particle was about  $450 \text{ nm}$ , and its depth was about  $18 \text{ nm}$ . Thus, for a given laser fluence, the smaller the particle of the monolayer on the surface, the smaller and shallower the created hole. In addition, when the particle size is kept constant and the laser fluence increases, the created hole becomes larger and deeper.

The calculation of the near-field light intensity is based on the solution of the boundary-value problem for a spherical particle on a flat semi-infinite substrate. Recently, an appropriate method was developed to solve this problem in our previous paper [17]. The accurate solution can be derived using this method. The electromagnetic field is the sum of both the scattered field and the incident field. The calculation shows that the multi-reflection of the Poynting vector between the particle and the substrate results in a higher intensity on the contact area, and the full-width at the half-maximum for the intensity distribution is even smaller than that from the Mie solution. For a non-absorptive spherical particle, incident light could excite some resonance modes inside the particle, as well as produce enhanced light intensities near the contact area. In this case the particle acts like a lens, as was shown in [12, 13, 17, 18]. It is assumed that the incident plane wave is normalized to unity, the wave propagates along the  $z$ -coordinate, the electric vector is along the  $x$ -coordinate, and the magnetic vector is along the  $y$ -coordinate. Figure 4 shows the calculated field intensity at the contact point between the particle and the magnetic surface. The particle is  $1.0 \mu\text{m}$  in diameter. The contact point is set to be  $(0,0)$ . The relative field intensity and its contour in the area of  $-0.30 \mu\text{m} \leq x \leq 0.30 \mu\text{m}$ ,  $-0.30 \mu\text{m} \leq y \leq 0.30 \mu\text{m}$  is clearly shown in Fig. 4. It is shown that, when the laser irradiates normally to the substrate, the laser fluence near the contact area is greatly enhanced and a main resonance is confined in a region less than  $200 \text{ nm}$  in size. An intensity distribution along the  $z$ -axis and for  $x = 0$ , calculated from Mie

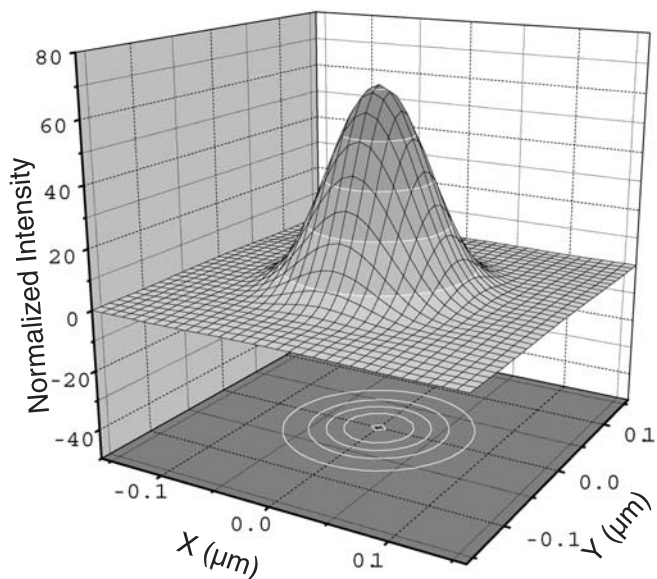


**FIGURE 4** 3-D calculated field intensity at the contact point between a particle with a size of  $1.0 \mu\text{m}$  and the Ni surface

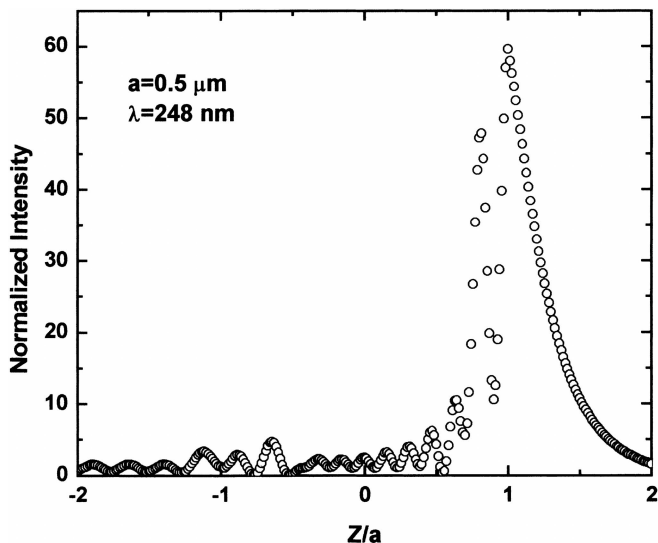


**FIGURE 5** Calculated field intensity distribution along the  $z$ -axes for  $x = 0$ , where  $a$  is the radius of the particle

theory, is shown in Fig. 5. From this figure, there is a maximal light enhancement at  $z = a$ , where  $a$  is the radius of the particles.

The origin of the light enhancement is the excitation of optical resonance modes in the particles [19, 20]. The light enhancement is very sensitive to the size parameter. Figure 6 displays the calculated field intensity and its contour for the case of a particle size of  $0.5 \mu\text{m}$ . Comparing the two cases of particle sizes of  $1.0 \mu\text{m}$  and  $0.5 \mu\text{m}$ , shown in Figs. 4 and 6, respectively, both main resonance modes occur in a region less than  $200 \text{ nm}$  in size. The maximal light enhancement of the former is more than three times larger than that of the latter. With a low laser fluence of  $150 \text{ mJ/cm}^2$  and a small particle  $0.5 \mu\text{m}$  in diameter, only a part of the main resonance light intensity near to the contact point  $(0,0)$  contributes to the creation of holes with sizes less than  $200 \text{ nm}$ , as shown in Fig. 3. With a high laser fluence of  $400 \text{ mJ/cm}^2$ , both the

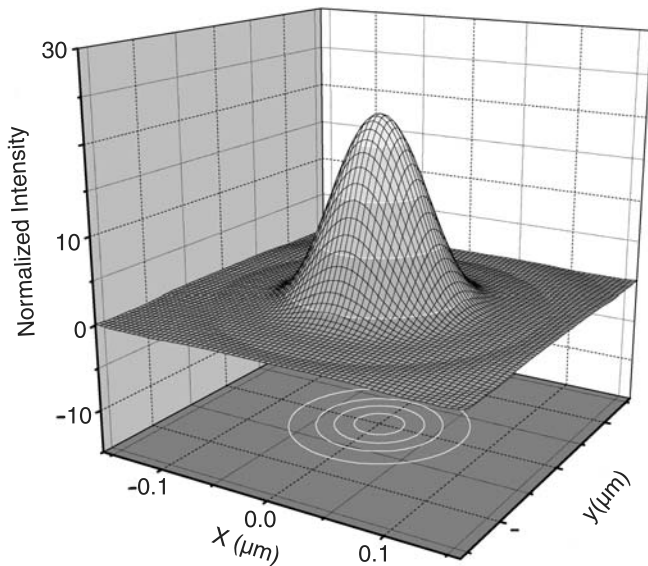


**FIGURE 6** 3-D calculated field intensity at the contact point between a particle with a size of  $0.5 \mu\text{m}$  and the Ni surface

whole main and side resonance modes can play a role in the formation of holes. Both contributions result in the formation of holes with sizes much greater than  $200 \text{ nm}$ , as shown in Fig. 2. Based on the configurations of the pits presented in the SEM images above, we could attribute the formation of these pits to the occurrence of rapid melting or evaporation in nanosized domains of the sample during laser irradiation. Combining this laser-assisted structuring surface method with self-organization processes, e.g., the utilization of 2-D colloidal monolayers [15, 16], will have important and exciting consequences for the structuring process, allowing the structuring of large substrate areas, and potentially resulting in a million and more holes for a laser single shot.

#### 4 Conclusions

Optical resonance and near-field effects in the interaction of particles on a substrate with laser light has been studied. Pits were created at the contact point between the transparent particles and the metallic surface by a single shot. The influence of particle size and laser fluence on the structuring of the surface was investigated. The morphologies of the created holes were characterized by AFM and SEM. With

a constant laser fluence, for two kinds of particles with diameters of  $0.5$  and  $1.0 \mu\text{m}$ , the created hole became smaller and shallower as the particle size decreased. When the particle size was kept constant, created holes became larger with higher laser fluence. For  $0.5\text{-}\mu\text{m}$  particles, with a fluence of  $150 \text{ mJ}/\text{cm}^2$ , the diameters and depths of the holes were about  $150 \text{ nm}$  and  $3.0 \text{ nm}$ , respectively. With a high fluence of  $400 \text{ mJ}/\text{cm}^2$  and for  $1.0 \mu\text{m}$  particle, the diameters and depths of the holes were about  $470 \text{ nm}$  and  $34 \text{ nm}$ . Theoretical calculations of the intensity distribution versus the particle size parameter in the contact area (substrate surface) were carried out. The calculation shows that, for a non-absorptive spherical particle, the incident light excites some resonance modes inside the particle and produces enhanced light intensities near the contact area. It is also shown that the light intensity near the contact area is non-uniform and sensitive to the particle size. The experimental results are explained well using the theoretical calculations.

#### REFERENCES

- 1 A.A. Gorbunov, W. Pompe: *Phys. Status Solidi* **145**, 333 (1994)
- 2 J. Jersch, K. Dickmann: *Appl. Phys. Lett.* **68**, 868 (1996)
- 3 Y.F. Lu, Z.H. Mai, G. Qiu, W.K. Chim: *Appl. Phys. Lett.* **75**, 2359 (1999)
- 4 S.M. Huang, M.H. Hong, Y.F. Lu, B.S. Luk'yanchuk, W.D. Song, T.C. Chong: *J. Appl. Phys.* **91**, 3268 (2002)
- 5 J. Jersch, F. Demming, K. Dickmann: *Appl. Phys. A* **64**, 29 (1997)
- 6 J. Jersch, F. Demming, L.J. Hildenhagen, K. Dickmann: *Appl. Phys. A* **66**, 29 (1998)
- 7 H.J. Mamin, P.H. Guethner, D. Rugar: *Phys. Rev. Lett.* **65**, 2418 (1990)
- 8 R. Huber, M. Koch, J. Feldmann: *Appl. Phys. Lett.* **73**, 2521 (1998)
- 9 J. Boneberg, H.-J. Münzer, M. Tresp, M. Ochmann, P. Leiderer: *Appl. Phys. A* **67**, 381 (1998)
- 10 D.R. Halfpenny, D.M. Kane: *J. Appl. Phys.* **87**, 6641 (1999)
- 11 D.M. Kane, D.R. Halfpenny: *J. Appl. Phys.* **87**, 4548 (2000)
- 12 M. Mosbacher, H.-J. Münzer, J. Zimmermann, J. Solis, J. Boneberg, P. Leiderer: *Appl. Phys. A* **72**, 41 (2001)
- 13 Y.F. Lu, L. Zhang, W.D. Song, Y.W. Zheng, B.S. Luk'yanchuk: *JETP Lett.* **72**, 457 (2000)
- 14 S. Hayashi, Y. Kamamoto, T. Sutuki, T. Hirai: *J. Colloid Interface Sci.* **144**, 538 (1991)
- 15 M. Mosbacher, N. Chaoui, J. Siegel, V. Dobler, J. Solis, J. Boneberg, C.N. Afonso, P. Leiderer: *Appl. Phys. A* **69**, S331 (1999)
- 16 F. Burmeister, C. Schäfle, B. Keilhofer, C. Bechinger, J. Boneberg, P. Leiderer: *Adv. Mater.* **10**, 495 (1998)
- 17 B.S. Luk'yanchuk, Y.W. Zheng, Y.F. Lu: *Proc. SPIE* **4065**, 576 (2000)
- 18 P. Leiderer, J. Boneberg, V. Dobler, M. Mosbacher, H.-J. Münzer, N. Chaoui, J. Siegel, J. Solis, C.N. Afonso, T. Fourier, G. Schrems, D. Bäuerle: *Proc. SPIE* **4065**, 249 (2000)
- 19 P. Chylek, J.T. Kiehl, M.K. Ko: *Phys. Rev.* **18**, 2229 (1978)
- 20 A. Ashkin, J.M. Dziedzic: *Appl. Opt.* **20**, 1803 (1981)